



***The World's Largest Open Access Agricultural & Applied Economics Digital Library***

**This document is discoverable and free to researchers across the globe due to the work of AgEcon Search.**

**Help ensure our sustainability.**

Give to AgEcon Search

AgEcon Search  
<http://ageconsearch.umn.edu>  
[aesearch@umn.edu](mailto:aesearch@umn.edu)

*Papers downloaded from AgEcon Search may be used for non-commercial purposes and personal study only. No other use, including posting to another Internet site, is permitted without permission from the copyright owner (not AgEcon Search), or as allowed under the provisions of Fair Use, U.S. Copyright Act, Title 17 U.S.C.*

*No endorsement of AgEcon Search or its fundraising activities by the author(s) of the following work or their employer(s) is intended or implied.*

# Multitemporal distribution analysis of *Dodonaea viscosa* (L.) Jacq. by remote sensing in Durango, Mexico

Márquez-Linares, Marco, A.<sup>1</sup>; Escobar-Flores, Jonathan G.<sup>1\*</sup>; Sandoval, Sarahi<sup>2</sup>; Pérez-Verdín, Gustavo<sup>1</sup>

<sup>1</sup> Instituto Politécnico Nacional, Centro Interdisciplinario de Investigación para el Desarrollo Integral Regional, Unidad Durango, Durango, México, C.P. 34220. <sup>2</sup>CONACYT-Instituto Politécnico Nacional, CIIDIR, Unidad Durango, Durango, México, C.P. 34220.

\*Autor para correspondencia: jescobarf@ipn.mx

## ABSTRACT

**Objective:** to determine the distribution of *D. viscosa* in the vicinity of the Guadalupe Victoria Dam in Durango, Mexico, for the years 1990, 2010 and 2017.

**Design/Methodology/Approach:** Landsat satellite images were processed in order to carry out supervised classifications using an artificial neural network. Images from the years 1990, 2010 and 2017 were used to estimate ground cover of *D. viscosa*, pastures, crops, shrubs, and oak forest. This data was used to calculate the expansion of *D. viscosa* in the study area.

**Results/Study Limitations/Implications:** the supervised classification with the artificial neural network was optimal after 400 iterations, obtaining the best overall precision of 84.5 % for 2017. This contrasted with the year 1990, when overall accuracy was low at 45 % due to less training sites (fewer than 100) recorded for each of the land cover classes.

**Findings/Conclusions:** in 1990, *D. viscosa* was found on only five hectares, while by 2017 it had increased to 147 hectares. If the disturbance caused by overgrazing continues, and based on the distribution of *D. viscosa*, it is likely that in a few years it will have the ability to invade half the study area, occupying agricultural, forested, and shrub areas.

**Keywords:** supervised classification, land cover, land change detection, invasive species, GIS

## INTRODUCTION

*Dodonaea viscosa* (L.) Jacq (Sapindaceae) is an evergreen shrub with wide distribution in Mexico and the world, thereby considered to be a cosmopolitan species (Harrington, 2008). It inhabits areas affected by livestock production or other disrupting factors in tropical or subtropical zones in Mexico (Rzedowsky, 1978); it is known by many names (Acosta, 2014), and in the study area as jarilla. In the state of Durango, Mexico, its presence has been detected along the eastern flanks of the Sierra Madre Occidental and in the San Pedro river basin (González-Elizondo et al., 2007), where it possibly spilled over from subtropical zones to temperate climate zones, invading transition areas along the eastern flank of the Sierra Madre Occidental. Due to its capacity to colonize disturbed areas, extensive areas can be found where this species is dominant, forming densely populated communities. Acosta (2016) studied the successional role of *D. viscosa* in Durango, finding that it is not an inhibiting species since it coexists with many others; however, wherever it establishes

itself, floristic diversity decreases. Landowners and ejidatarios (community landowners) have seen how this species reduces grass production on lands where extensive grazing activities take place, thus notably affecting livestock production. According to individual observations, wherever the shrub becomes established it begins an expansion process toward nearby zones, forming dense communities where livestock do not graze, being an unpalatable species for them (CONAFOR, 2019). The objective of this study was to determine the expansion potential of *D. viscosa* once it begins to establish itself in a specific area. The study was carried out in the areas surrounding the Guadalupe Victoria Dam in the municipality of Durango, Mexico, for the years 1990, 2010 and 2017. To this end, several areas with presence of this species were studied and satellite images from the Landsat platform were retrospectively analyzed to determine the rise or decline of this plant and the possible factors that allow its dispersal in time, as well as to contribute to preventing its dispersal.

## MATERIALS AND METHODS

To evaluate the changes in *D. viscosa* distribution throughout several decades, the area surrounding the Guadalupe Victoria Dam in Durango, Mexico, was selected. This dam's catchment area is located to the west of Durango City ( $104^{\circ} 48.182'$  and  $104^{\circ} 43.912'$  W, and  $23^{\circ} 51.478'$  and  $23^{\circ} 58.120'$  N) at an altitude between 1940 m and 2260 m, covering an area of 2,700 ha with secondary shrubland, oak-pine forest, grasslands, and *D. viscosa* shrubs (INEGI, 2018a). It has a semidry temperate climate with summer rains; temperatures fluctuate between 16 and 18 °C and precipitation is approximately 500 mm (INEGI, 2018b). This area was selected because of observations that the distribution of *jarilla* has increased gradually within it.

### Image acquisition and processing

Landsat-4 TM, Landsat-5 TM, and Landsat-8 OLI satellite images were used from the first days of the month of October, from years 1990, 2010 and 2017, which were downloaded free of charge from the United States Geological Survey (available at <http://glovis.usgs.gov/>). These images were used to carry out a supervised classification to identify six different types of ground cover, which were: secondary scrubland (Ms), grassland (Ps), cropland (Cul), oak-pine forest (Bqp), bodies of water (Ag), and areas with *D. viscosa*. The first categories are classifications made by the INEGI (National Institute of Statistics and Geography) for their land use and vegetation maps. Only *D. viscosa* was added, since it is the subject of this study and for having particular reflectance traits due to the yellowish-green color of its leaves. A back propagation artificial neural network (BPNN) was used for the supervised classification (SNAP, 2017). BPNN is widely used due to its structural simplicity and robust modelling of non-linear connections. The BPNN comprised a set of three layers (raster): an input layer, a hidden layer, and an output layer (Richards, 1999). Each layer is a series of parallel processing elements (neurons or nodes). Each one of a layer's nodes is linked to all the nodes of the following layer (Guo et al., 2013).

The first step in BPNN supervised classification was to enter the input layer, which corresponded to the pixel values of the Landsat satellite bands. Then

weights were assigned to the BPNN to produce analytic data based on the input values. These data were contrasted with the category to which each training pixel belonged, corresponding to georeferenced sites (Datum, WGS-84, 13N). A random stratified sampling method (Olofsson et al., 2013) was used to generate the reference data in the QGIS software (QGIS Development Team 2016). The 1990 training areas were obtained from the land use and vegetation map from INEGI's series II. For 2010, the IV series was used, and for 2017, 300 entries from the field and 19 entries from the Northeastern Mexican herbalist network's database ([www.herbanwmex.net](http://www.herbanwmex.net)) were used. A total of 1,644 random points were sampled (Goodchild et al., 1994). The number of classes were: i) *D. viscosa*, 342 sites; ii) secondary shrubland, 382 sites; iii) oak-pine forest, 212 sites; iv) grassland, 419 sites; v) crops, 180 sites; and vi) water, 109 sites.

The class discrimination processes happened in the hidden layer, and the synapses between layers were identified through an activation function. A logistic function was used as well as a training rate of 0.20 (Hepner et al., 1990; Richards, 1993; Braspenning and Thuijsman, 1995). Learning occurs when adjusting the weights in the node to minimize the difference between the activation of the output node and the BPNN, then calculating the error in each iteration with the root-mean-square error (RMS). The output layer consisted of six neurons that represent the six classes of ground cover considered. Once the classifications of each of the Landsat images were achieved, changes in each class were detected through the Change Detection

algorithm with the Environment for Visualizing Images (ENVI)<sup>®</sup> software. The image designated as the initial state corresponded to the year 1990 and the final states were the images from 2010 and 2017. A change matrix was generated, with which the surface areas that were substituted by *D. viscosa* were calculated for each of the classes of vegetation ground cover.

### Classification accuracy

For the classification validation process, confusion matrixes were applied and analyzed with the procedure proposed by Jensen (1986), which is the most commonly used method for calculating the accuracy of global classification. This consists in calculating the omission and commission errors in order to calculate the percentage of error and its confidence limits, both for the total classification and for each category. For the image from 1990, 348 verification sites were used; for 2010, 1,646 sites were used; and for 2017, 2,099 sites were used.

## RESULTS AND DISCUSSION

The best results for the supervised classifications by the BPNN algorithm were obtained after 400 iterations with learning rate values (RMS) of less than 0.08 and a global accuracy of 84.5 % (Figure 1).

In the dispersion diagram, when comparing the red band versus the infrared band (NIR) of the OLI sensor for *D. viscosa* reflectance evidence, it was found that this species' pattern had a very low reflectance percentage in the red band (10 %) and a mid-range reflectance percentage in the infrared band (35 %). This was very useful for the separability of the classes considered (Figure 2).

In the 1990 image, classification accuracy was 44.5 %, which is very low. However, given that INEGI

map data were used (series II land use and vegetation) as well as existing collection data for that year, it was difficult to improve accuracy given the antiquity of the information. This table also shows that the *D. viscosa* class is confused with the shrubland class and the Bqp class (omission). However, the shrubland class is primarily confused with *D. viscosa* (commission). The total area covered by *D. viscosa* in 1990 (Table 1) was 6.8 ha, and according to Figure 3, it was found only in the southern part of the study area. On the other hand, the largest area corresponded to the shrubland class with 1289.8 ha. Agriculture covered a surface area of 284.7 ha, grassland covered 224.7 ha, and Bqp covered 577.6 ha.

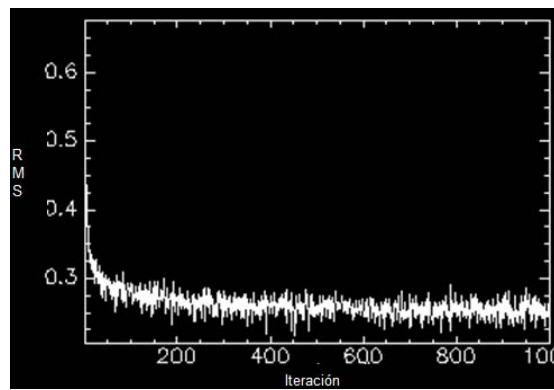


**Figure 1.** Diagram showing BPNN learning; a simulation of less than 500 iterations is sufficient to achieve the supervised classification.

viscosa increased to 147.5 ha, showing a dotted patch distribution. The surface areas covered by the rest of the classes were: shrubland, 1491.7 ha; cropland, 382.4 ha; grassland, 232.7 ha; and Bqp, 314.2 ha. The image from 2017 had a classification accuracy of 87 % due to an improved sensor and improved field verification points, and not with INEGI maps. Table 3 shows that *D. viscosa* is confused mostly with Bqp (omission) by 5.8 %, and the rest of the classes are confused with *D. viscosa* (commission) by 20.4 %. The surface area covered by this species rose to 222.0 ha. Its distribution is also in patches, although larger in size in relation to the image from 2010. The areas covered by shrubland were 1484 ha; cropland, 164.4; grassland, 314.2 ha;

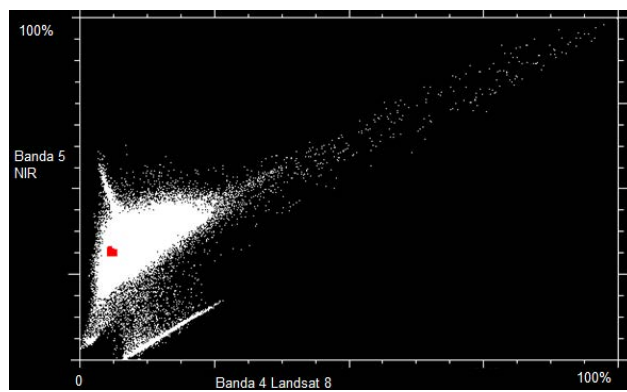


**Figure 2.** Diagram of the dispersion of *D. viscosa* reflectance values. The red point shows the convergence point between both bands.

**Table 1.** Contingency and errors for the 1990 classification. Total classification accuracy of 44.5%.

Class	D. visc	SM	CRP	Gr	OPF	TOTAL	Omission error	% Omission error	Commission error	% Commission error	Surface (ha)
1. <i>D. viscosa</i>	38	10	0	0	28	76	38	0.50	5	0.07	6.8
2. SM	5	51	25	59	47	187	136	0.73	15	0.08	1289.8
3. CRP	0	0	16	0	0	16	0	0.00	29	1.81	316.4
4. Gr	0	2	1	23	13	39	16	0.41	62	1.59	577.6
5. OPF	0	3	0	0	27	30	3	0.10	88	2.93	224.7
TOTAL	43	66	42	82	115	348	193		199	0.57	2415.3

\*SM=Secondary scrub, crp=Crops, GR=Grassland, OPF=Oak-pine forest.

**Table 2.** Contingency table and errors for the 2010 classification. Overall Accuracy of 75.6%.

Class	D. visc	SM	CRP	Gr	OPF	TOTAL	Omission error	% Omission error	Commission error	% Commission error	Surface (ha)
1. <i>D. viscosa</i>	132	8	21	0	68	229	97	0.42	38	0.17	114.5
2. SM	0	201	4	89	83	377	176	0.47	39	0.10	1491.7
3. CRP	22	16	406	0	5	449	43	0.10	33	0.07	164.4
4. Gr	16	15	8	401	11	451	50	0.11	91	0.20	314.1
5. OPF	33	0	0	2	105	140	35	0.25	167	1.19	232.7
TOTAL	8	401	442	496	277	1646	401		368	0.22	2317.7

\*SM=Secondary scrub, crp=Crops, GR=Grassland, OPF=Oak-pine forest.

**Table 3.** Contingency table and errors for the 2017 classification. Overall accuracy of 85.4%.

Class	D. visc	SM	CRP	Gr	OPF	TOTAL	Omission error	% Omission error	Commission error	% Commission error	Surface (ha)
1. <i>D. viscosa</i>	342	2	0	0	19	363	21	0.06	74	0.20	147.0
2. SM	24	619	119	2	0	764	145	0.19	20	0.03	954.1
3. CRP	50	0	348	7	0	405	57	0.14	141	0.35	434.5
4. Gr	0	0	20	418	0	438	20	0.05	11	0.03	374.8
5. OPF	15	18	2	2	92	129	37	0.29	19	0.15	390.7
TOTAL	431	639	489	429	111	2099	280		265	0.13	2301.1

\*SM=Secondary scrub, crp=Crops, GR=Grassland, OPF=Oak-pine forest.

and Bqp, 232.7 ha (Figure 3 and Figure 4).

As shown in Tables 1 and 3, as well as Figure 4, *D. viscosa* has gradually increased its ground cover. Figure 3 demonstrates how *D. viscosa*, after establishing itself in a small area, begins to spread out from its original point; this was particularly evident

in the changes seen from 2010 to 2017. Table 1 shows that in 1990, *D. viscosa* covered a limited area of 6.8 ha, and most of the surface corresponded to shrubland. For the year 2010, the area covered by *D. viscosa* increased to 114.5 ha, and for the year 2017, it increased to 147.0 ha. Figure 3 shows how in 1990, the species was limited to a small

location to the south of the study area. In 2010, its distribution had grown to small patches throughout the whole area. However, by 2017 these patches had spread out to form denser and more extensive stretches. Comparing the *D. viscosa* distribution map of 1990 and 2010 with its distribution in 2017, as well as with its expansion rate, the results

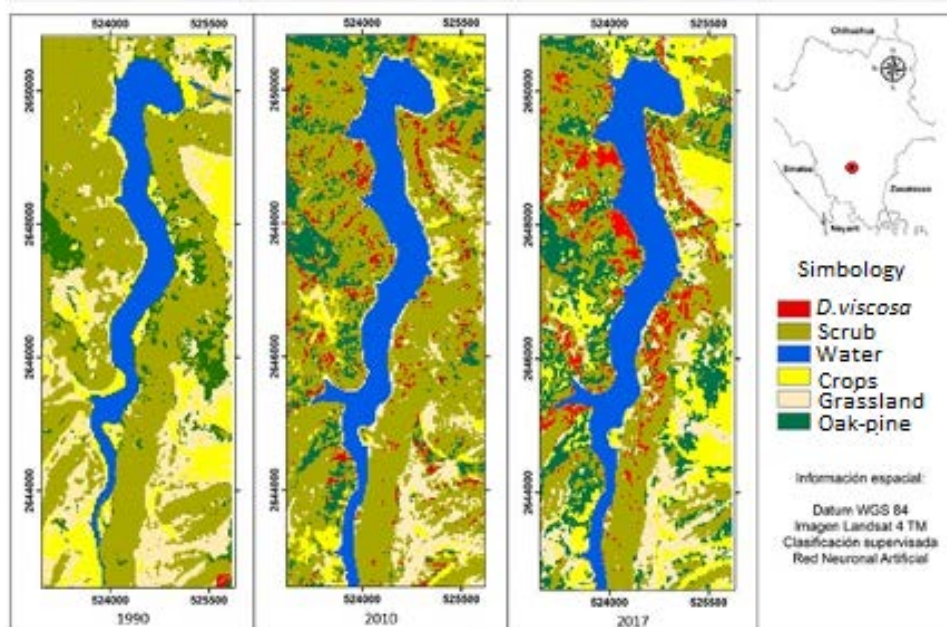


**Figure 3.** Distribution of *D. viscosa* in the years 1990, 2010, and 2017 within the catchment area of the Guadalupe Victoria Dam in Durango, Mexico (Datum: WGS 81, UTM Projection, Geographic zone UTM13N).

suggest that without implementing measures to prevent its spread, in a few years the species could completely replace native vegetation. This has happened in other nearby locations in the south of the state of Durango, where the dominance of this species can be observed in large extensions of land (Acosta, 2016).

*Dodonaea viscosa* is considered to be an invasive species thanks to its ability to colonize sites outside of its original distribution area (González Elizondo, 2007; Acosta, 2016). Because of its widespread distribution in all of Mexico and since it is considered native in tropical and subtropical zones, it is not deemed an invasive species in some studies, but rather a native plant that colonized disturbed areas (CONABIO, 2009; Richardson, 2011).

This was the case in the study area, where the presence of this species in 1990 was rare or limited to a very specific site to the south of the area. Nevertheless, in 2010 the plant was apparent in patches throughout practically the entire area; from these it then spread out, resulting in larger and more densely covered areas, as can be seen in the 2017 image. This signified a gradual increase of 6.75 ha in 1990 to 114.5 ha in 2010, and to 147.0 ha in 2017, that is, 77.9 % more in the last seven years. The rapid spread of jarilla in the study area can be attributed to extrinsic or intrinsic factors. On the extrinsic side, it should be recalled that the area is subject to extensive unregulated grazing that has caused sheet erosion, rock exposure, and

vegetation disturbance, creating an attractive environment for the plant's establishment just as several authors have proposed, indicating that the plant is generally found in sites distressed by erosion, fires or overgrazing (Rzedowski, 1978; González Elizondo et al., 2005 and 2007; Acosta, 2016; and Rivas González, 2019).

Authors like Acosta (2016) suggest that *D. viscosa* takes part in the first stages of ecological succession in the recovery of original vegetation; however, the findings of this study reveal that instead it replaces the original vegetation, especially shrublands where it settles and spreads.

Given this circumstance, and considering that disturbances from grazing and fire of the site will probably continue, it is possible that jarilla will keep increasing its populations, establishing a state of disclimax that will remain as long as the disturbance conditions do not change.

In terms of the plant's intrinsic factors, wind dispersion of the seed (winged seeds) and germination mechanisms with no need for scarring processes (CONAFOR, n.d.) suggest that its establishment is facilitated in areas with sites exposed to bare ground like those of the study area, subject to extensive grazing, sheet erosion, rock

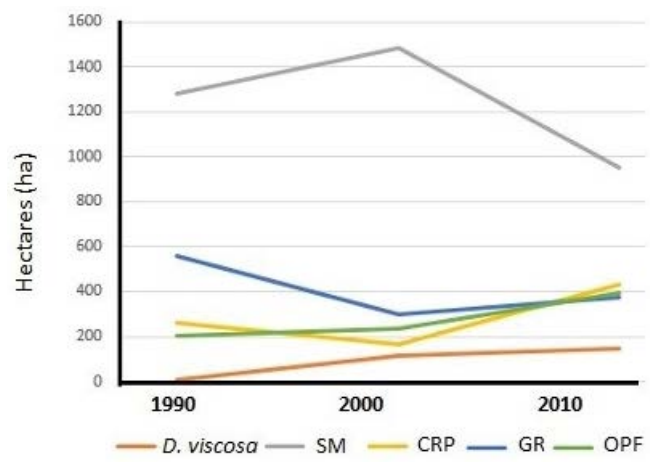


**Figure 4.** Changes in the ground cover of the Guadalupe Victoria Dam river basin. M. sec = Secondary shrubland, Bqp=Oak-pine forest.

exposure, and occasional fires. The seed's small size ( $\pm 1$  mm) and its lack of nutritional reserves are typical of ruderal species (Grime, 2001), which adapt to disturbed sites with unlimited resources. Diverse studies (Jurado and Wstoby, 1992) of other species have shown that the size of the seed and its nutritional reserves are important to determine "safe" sites for their establishment. This contrasts with the case of plants with large seeds and nutritional reserves, such as oaks, which can remain viable for some time in wait of favorable environmental conditions for its establishment and survival. Unlike these species, those with seeds that have no reserves must find adequate conditions quickly to take root or otherwise the propagule dies for lack of nutrients (Fenner, 2000).

It is highly probable that jarilla was not present in 1990 in the southern part of the study area, given that site has an altitude of approximately 2225 m, at which annual frosts are frequent and intense, impeding the vegetative development of the plant in the long term. Figure 5 demonstrates an intense frost at the

start of 2017 and how it dried out the plant, but later resprouted from the base. This indicates that an important limitation to the distribution and spread of the plant is the zone where strong annual frosts begin, which impede or limit vegetative development. Figure 5 shows the area covered by *D. viscosa*.

Concerning thematic classifications, there was clear improvement between the 1990 classification, with a global precision of 44.5 %, and the 2017 classification, with a global precision of 85.4 %. This can be due to two factors. i) Radiometric resolution, referring to the number of digital levels used to express the data obtained from the sensor (Chuvieco, 2010); in the 1990 image, the TM sensor uses 8 bits, which results in 256 digital levels, while the 2017 image corresponds to the OLI sensor, which has a 12-bit storage capacity, that is, it can capture on 4,096 digital levels, making it 20 times more sensitive than a TM image (Chi, 2013). ii) Spatial resolution; it is possible that in the 1990 classification, the populations of *D. viscosa* covered a surface area of less than 10 m<sup>2</sup>, while the minimum pixel size of the Landsat multispectral images is 30 m<sup>2</sup>, and thus detection was not viable. The opposite case occurred in the 2017 image, where *D. viscosa* populations surpassed two hectares per location.

## CONCLUSIONS

### The study

area of *D. viscosa* has high potential for the species to spread and replace cropland, grassland, scrubland, and some oak-pine forests, having occupied 6.7 ha in 1990, 114 in 2010, and 147 in 2017. Given that the potential distribution sites in the study area are very extensive, it is probable that this plant's expansion will continue to climb in light of the disrupting conditions that are common in these locations. *D. viscosa* is a plant that can disperse and spread very quickly due to the properties of its seed, including its capability of wind dispersal and easy germination. The limiting factor in its distribution seems to be extremely cold conditions, which are more frequent and intense as the altitude rises. The invasive potential of viscosa is very high; if climate change reduces the frequency of frosts and brings about a rise in temperature, combined with continuous disturbances of vegetation from human activity, it is to be expected that this plant will notably increase its distribution toward higher altitudes and latitudes.

## REFERENCES

Acosta H. A. C., González-Elizondo M. y Ruacho-González L. (2014). Conocimiento actual de *Dodonea viscosa* (SAPINDACEAE) en Durango: Una Revisión. *Vidsupra visión Científica*, 6(1), 19-22

Acosta H. A. (2016). Papel sucesional de *Dodonea viscosa* en la cuenca alta del río San Pedro Mezquital (Tesis de Maestría). Instituto Politécnico Nacional, CIIDIR, Durango.

Braspenning P. J. y Thuijsman F. (1995). Artificial neural networks: an introduction to theory and practice. USA. Springer Science & Business Media.

CONABIO. (2009, 30 de junio). Malezas de México. Recuperado de <http://www.conabio.gob.mx/malezasdemexico/sapindaceae/dodonea-viscosa/fichas/ficha.htm>



**Figure 5.** An image of *D. viscosa* resprouting from dried plants during the 2017 frost.

CONAFOR. (2019, 17 de octubre). *Dodonea viscosa* L. Jacq. Recuperado de <http://www.conafor.gob.mx:8080/documentos/docs/13/918Dodonea%20viscosa%20.pdf>.

Chi, J. (2013). Validation of the radiometric characteristics of Landsat 8 (LDCM) OLI Sensor using band aggregation technique of EO-1 Hyperion hyperspectral imagery. *Korean Journal of Remote Sensing*, 29(4), 399-406.

Chuvieco, E. (2010). *Teledetección ambiental. La observación de la tierra desde el espacio*. Primera edición. Editorial Ariel. Barcelona, Espana. 568 p.

Feener M. (2000). *Seeds: The ecology of regeneration in plant communitis*. N.Y., EUA: CABI publishing

González E. M. S., González E. M., López E. I. L., Tena F. G. y Márquez-Linares M. A. (2005). Cambios y tendencias sucesionales en ecosistemas de Durango. *Vidsupra*, 1(1), 5-11.

González E. M. S., González E. M., Márquez-Linares M. A. (2007). *Vegetación y ecorregiones de Durango*. México, D.F.: Editorial Plaza y Valdez

Goodchild M. F. (1994). Integrating GIS and remote sensing for vegetation analysis and modeling: methodological issues. *Journal of Vegetation Science* 5:615-626. doi: 10.2307/3235878.

Grime, J. P. (2006). *Plant strategies, vegetation proces and ecosystem properties*, 2nd Ed. U.S.A: Chichester

Guo P. T, Wu W., Sheng Q. K, Li MF, Liu H. B and Wang Z. Y. (2013). Prediction of soil organic matter using artificial neural network and topographic indicators in hilly areas. *Nutrient cycling in agroecosystems* 95:333-344. doi: 10.1007/s10705-013-9566-9.

Hamlyn G.J. y Vaughan R. A. (2010). *Remote sensing of vegetation, principles, techniques, and application*. N.Y, EUA: Oxford

Harrington M. (2008). *Phylogeny and evolutionary history of Sapindaceae and Dodonea*. (PhD Thesis). James Coock University. Australia.

Hepner G, Logan T, Ritter N, Bryant N. 1990. Artificial neural network classification using a minimal training set. Comparison to conventional supervised classification. *Photogrammetric Engineering and Remote Sensing*. 56(4): 469-473.

INEGI (2018a). Conjunto de datos vectoriales de información topográfica F13B11 Presa Guadalupe Victoria escala 1:50000 serie III. Recuperado de <https://www.inegi.org.mx/app/biblioteca/ficha.html?upc=702825271718>

INEGI (2018b). *Climatología serie I. Esc 1:1,000,000*

Jensen R. J. (1986). *Digital image processing*. N. J., EUA: Prentice-Hall

Jurado E. y Westoby M. (2002). Seedling growth in relation to seed size among species of arid Australia. *Journal of ecology*. 80, 407-416.

Olofsson P., Foody G.M., Herold M., Stehman S.V., Woodcock C.E. y Wulder M.A. (2013). Good practices for estimating area and assessing accuracy of land change. *Remote Sensing of Environment* 148, 42-57. doi: 10.1016/j.rse.2014.02.015

Richards J. A. (1999). *Remote Sensing Digital Image Analysis*, Berlin, Alemania, Springer-Verlag.

Richardson D.M., Pysek P. y Carlton J.Y. (2011). A compendium of essential concepts and terminology in biological invasions. En D.M. Richardson. (Ed.), *Fifty years of invasion ecology: the legacy of Charles Elton* (pp. 409-420). Oxford, UK: Black Well.

Rivas G. R. (2019). Disturbios y variables ambientales asociados a la presencia de *Dodonea viscosa* en los municipios de Durango y Mezquital, Durango. (Tesis Maestría). Instituto Politécnico Nacional, CIIDIR-Dgo. Durango, México.

Richards J. A. (1999). *Remote Sensing Digital Image Analysis*. Berlin: Ed. Springer-Verlag

Rzedowsky, J. (1978). *Vegetación de México*. México D.F. Ed. Limusa.